Nuclear structure of ^{17}Ne by the three-neutron pickup (^{3}He,^{6}He) reaction

V. Guimarães,[1,2] S. Kubono,[2] N. Ikeda,[3] I. Katayama,[2] T. Nomura,[4] M. H. Tanaka,[4] Y. Fuchi,[4] H. Kawashima,[4] S. Kato,[4] H. Toyokawa,[5] C. C. Yun,[6] T. Niizeki,[7] T. Kubo,[8] M. Ohura,[8] and M. Hosaka[9]

[1]*Department of Physics, University of Notre Dame, Notre Dame, Indiana 46556*

[2]*Center for Nuclear Study, University of Tokyo, 3-2-1 Midori-cho, Tanashi, Tokyo 188, Japan*

[3]*Department of Physics, Kyushuu University, Fukuoka, Japan*

[4]*Institute of Particle and Nuclear Physics, KEK, Tsukuba 305, Japan*

[5]*Research Center for Nuclear Physics, Osaka 567, Japan*

[6]*Department of Physics, Tohoku University, Sendai 980, Japan*

[7]*Tokyo Institute of Technology, Meguro, Tokyo 152, Japan*

[8]*Institute of Physical and Chemical Research (RIKEN), Wako, Saitama 351-01, Japan*

[9]*Institute for Molecular Science, Okazaki 444, Japan*

(Received 11 February 1998)

The nuclear structure of ^{17}Ne has been studied by the ^{20}Ne(^{3}He,^{6}He)^{17}Ne reaction at 70 MeV. Thirteen levels were identified in ^{17}Ne, and angular distributions have been measured for the first time for this reaction. Based on the observed transferred angular momentum dependence of the angular distributions, a spin-parity assignment has been made for several states in ^{17}Ne. With the inclusion of the data on ^{17}Ne, $T=\frac{3}{2}$ quartet analog states have been completed for six levels in the $A=17$ isobar system. The level shifts in these $A=17$ nuclei are analyzed in terms of the isobaric multiplet mass equation (IMME). The results of such an analysis show a slight linear dependence of the b and c coefficients of the equation on the excitation energy. The coefficients for the positive parity states seem to follow a different systematics than the negative parity states, suggesting that these parity-dependent level shifts are reflecting the structure change. These coefficients of the IMME are discussed. [S0556-2813(98)01707-5]

PACS number(s): 21.10.Hw, 25.55.Hp, 27.20.+n

I. INTRODUCTION

The structure of nuclei near the drip lines is one of the major concerns in nuclear physics. Although the proton drip line for light mass nuclei is well established, a detailed investigation of their properties is still necessary. Also, the discovery of extended tails of nuclear matter for weakly bound nuclei on the neutron-rich side has prompted a search for weak binding effects also in proton-rich nuclei. Among the $A=17$ isobar, several authors have pointed out that ^{17}F is a good candidate for proton-halo formation [1] since the proton separation energy is only 0.60 MeV. However, no strong experimental evidence has been observed so far. On the other hand, the largest interaction radius observed for ^{17}Ne [2] among the $A=17$ isobar suggests that this nucleus could have a proton halo. Thus, to get better insight into the structure of the ^{17}Ne we studied excited states up to 6.4 MeV in this nucleus. The level shift of the first $\frac{1}{2}^{+}$ state in ^{17}Ne is investigated, and the systematic behavior in energy of this state in the $N=7$ isotone is discussed in connection with a possible proton-halo formation.

Although a large number of $T=\frac{3}{2}$ states have been located in the other members of the $A=17$ multiplet, the level structure of the ^{17}Ne nucleus $T_z=-\frac{3}{2}$ was almost unknown with the exception of a few excited states that had been previously suggested [3,4]. Thus, the inclusion of the present data on the structure of ^{17}Ne also provides a good opportunity to make an extensive analysis in terms of the isobaric multiplet mass equation (IMME) for the four members of the $A=17$ system. Here we present an analysis on the systematics of the IMME coefficients for this system as a function of the excitation energy of ^{17}Ne. This is the first such analysis in a one multiplet system covering several excited states, and it can bring valuable spectroscopic information on the structure of $A=17$ nuclei.

The nuclear structure of ^{17}Ne was investigated here by the three-neutron pickup reaction ^{20}Ne(^{3}He,^{6}He)^{17}Ne. This reaction has been shown to be a useful spectroscopic tool, since the strong transferred angular momentum (L) dependence of the measured angular distributions allowed spin-parity assignment for the states [5]. Three-nucleon transfer reactions are experimentally difficult since the cross sections involved are generally very small. The development of a detector system including an accurate proportional gas counter [6] and a high-resolution magnetic spectrograph [7] has enabled measurements of extremely small cross sections of such reactions.

We report here on the experimental results and then on the detailed analysis of the nuclear structure of ^{17}Ne by the three-neutron pickup (^{3}He,^{6}He) reaction. Some of these results have been briefly reported before [8].

This paper is divided into the following sections. The experimental setup and the procedure are described in Sec. II, while the experimental results and the analysis in terms of the distorted wave Born approximation (DWBA) are reported in Sec. III. The interpretation of the level scheme of ^{17}Ne in terms of a large-base shell model is discussed in Sec. IV. In Sec. V, an analysis in terms of the IMME for the four members of the $A=17$ isobar system is presented. Section VI is devoted to the discussion of the level shift of the $\frac{1}{2}^{+}$ state. Finally, a summary is given in Sec. VII.

II. EXPERIMENT

The experiment was carried out with a sector-focusing cyclotron of the Center for Nuclear Study, University of Tokyo. The incident energy of the ^{3}He beam was 70.079 ± 0.050 MeV and the average current obtained was about 0.5 μA. The beam was transported into the scattering chamber, where a gas target system was mounted. The target system consisted of a gas cell and a ^{24}Mg metallic foil of 812 ± 20 μg/cm^2 thickness used for the energy calibration. The cell was filled with 99.95% isotopically enriched ^{20}Ne gas to a pressure of 21 cm Hg. In the measurements with the gas target, a rectangular double-slit system was used, defining the solid angle of 1 to 3 msr, depending on the detection angle.

The reaction products were momentum analyzed by a QDD-type magnetic spectrograph [7] and detected by a hybrid-type gas proportional counter [6], specifically designed to minimize the background for low-event rate experiments. A thin plastic scintillator was set just behind the proportional counter for energy and time-of-flight measurements.

The ^{6}He particles were identified using the energy signal from the plastic scintillator, energy loss from the proportional counter, and time-of-flight. The time-of-flight was obtained from the time interval between the cyclotron rf and the fast signal from the plastic scintillator. The vertical position, perpendicular to the directions of momentum dispersion as well as the particle trajectory, were also measured on the focal plane and used to reduce the background not arising from the target. Pileup rejection was applied by detecting two ΔE signals within 6 μs. Despite a moderate total counting rate (less than 5000 counts/s) this pileup rejection was still very useful to reduce the background since the cross sections of the (^{3}He,^{6}He) reaction are very small.

The momentum spectra of ^{6}He were measured at 12 angles between $\Theta_{lab} = 7.0°$ and 38.0°. The spectrum at $\Theta_{lab} = 10°$ was calibrated in energy using the known states of ^{21}Mg from the ^{24}Mg(^{3}He,^{6}He)^{21}Mg reaction [5] in the same experimental run. Using this calibration, the momentum spectra of all other angles were converted to energy spectra. A summed spectrum was obtained by adding all energy spectra for each angle normalizing each one for integrated charge, the effective target thickness, and solid angles. The summed spectrum of all spectra measured between $\Theta_{lab} = 7.0°$ and 29.0° is presented in Fig. 1(a). We also measured one spectrum at $\Theta_{lab} = 10.0°$ with a lower magnetic field. In this spectrum, shown in Fig. 1(b), we could observe some excited states with energy higher than 4 MeV. The overall energy resolution achieved was about 180 keV full width at half maximum (FWHM), mainly due to the energy loss difference of the ^{3}He beam and ^{6}He particles in the gas target system. The spectra were analyzed by fitting the shape of the peaks with a Gaussian function with exponential tails, where the parameters were obtained from the fitting of the ground-state peak. However, some peaks above the particle threshold energy have a slightly broader width.

III. EXPERIMENTAL RESULTS

The excitation energies and the uncertainties for the states observed in ^{17}Ne are listed in Table I. The uncertainties in

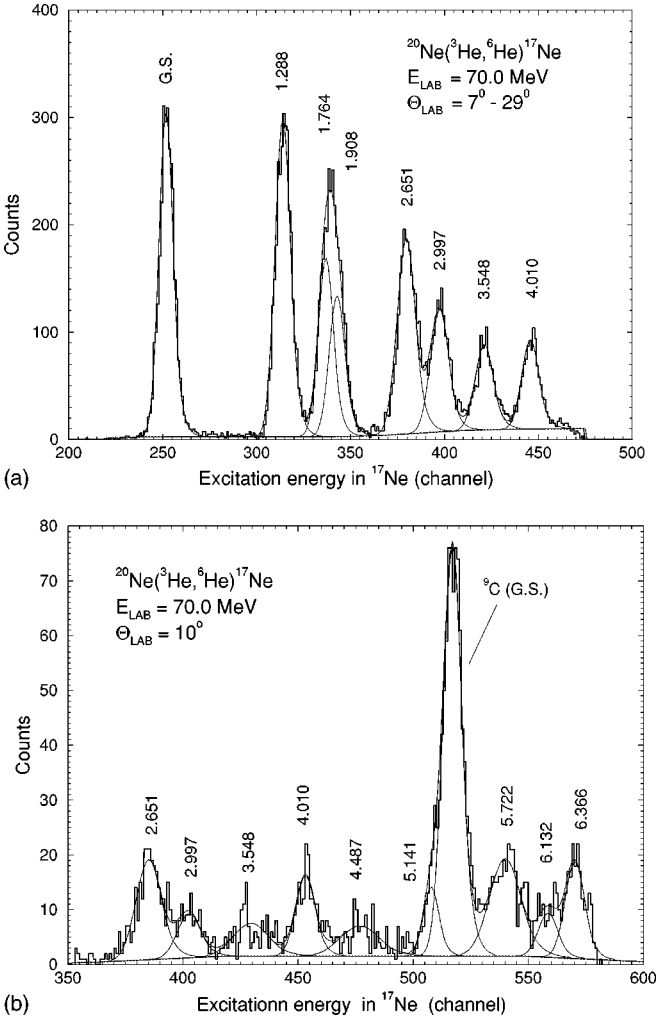

FIG. 1. (a) The summed ^{6}He energy spectrum from the ^{20}Ne(^{3}He,^{6}He)^{17}Ne reaction measured at $\Theta_{lab} = 7.0°$ to 29.0°. The excitation energies in ^{17}Ne are denoted. The solid lines indicate fits to individual peaks on a cubic polynomial background and the composite of the fits. (b) The spectrum obtained at $\Theta_{lab} = 10.0°$ with a lower magnetic field set. The excitation energies in ^{17}Ne between 2.5 and 6.4 MeV are denoted. The solid lines indicate fits to individual peaks on a background and the composite of the fits.

the values of the excitation energies were determined by taking into account all the experimental accuracies such as the uncertainty in the absolute energy of the incident beam, the effective target thickness, and the energy loss of the particles in the gas target. The accuracy of the Ziegler [10] empirical formulas used to calculate the energy loss of the particles was also taken into account. However, the major source of the uncertainties was due to peak centroid determination in the fitting procedure. The contribution of the uncertainty in the energy of the beam to the error of the excitation energies was very small (between 1 and 3 keV). There is an indication of a state at 5.141 MeV. However, since we cannot resolve this peak from the contamination peak of ^{9}C(g.s.), it has a large uncertainty. The present results on the excitation energies are in good agreement with, but much more accurate than the previously suggested values for ^{17}Ne [4], which are also listed in the table for comparison. The uncertainties on the experimental differential cross sections were obtained by taking into account most uncertainties; the statistical uncer-

TABLE I. Nuclear levels in ^{17}Ne identified. The accuracies in parentheses are in keV.

Ex. energy (MeV)	$\pm\Delta$Ex (keV)	L (DWBA)	J^π (DWBA)	J^π (IMME)	J^π adopted	Ex.[b] (MeV)	Ex.[c] (MeV)
0.0		1	$\frac{1}{2}^-,\frac{3}{2}^-$	$\frac{1}{2}^-$	$\frac{1}{2}^-$[a]		
1.288	8	1	$\frac{1}{2}^-,\frac{3}{2}^-$	$\frac{3}{2}^-$	$\frac{3}{2}^-$	1.35 (70)	1.284 (26)
1.764	12	3	$\frac{5}{2}^-,\frac{7}{2}^-$	$\frac{5}{2}^-$	$\frac{5}{2}^-$	1.84 (70)	1.754 (27)
1.908	15	0 (2)	$\frac{1}{2}^+,(\frac{3}{2}^+,\frac{5}{2}^+)$	$\frac{1}{2}^+$	$\frac{1}{2}^+$		1.916 (28)
2.651	12	(3,2)	$(\frac{5}{2}^-,\frac{7}{2}^-,\frac{3}{2}^+,\frac{5}{2}^+)$	$\frac{5}{2}^+$	$\frac{5}{2}^+$	2.77 (70)	2.619 (28)
2.997	11	3	$\frac{5}{2}^-,\frac{7}{2}^-$	$\frac{7}{2}^-$	$\frac{7}{2}^-$		3.006 (28)
3.548	20	5	$\frac{9}{2}^-,\frac{11}{2}^-$		$\frac{9}{2}^-$		
4.010	10	2	$\frac{3}{2}^+,\frac{5}{2}^+$		$\frac{3}{2}^+$		
4.487	22						
(5.141)	62					5.28 (90)	
5.722	23						
6.132	35						
6.366	22						

[a]From Ref. [9].
[b]From Ref. [4].
[c]Predictions by the IMME using the coefficients from Table IV.

tainties in the yield and the background under the peaks, target thickness, solid angle, and also uncertainties from the deconvolution of the doublet. The final values of the uncertainties were estimated to be about 10% for the forward angles to 30% for some states in the backwards angles of the corresponding absolute differential cross section.

A. Mass excess of ^{17}Ne

From the present work the mass excess of ^{17}Ne is determined to be 16.453 ± 0.032 MeV. In Table II it is compared with other experimental values [3,4] and with some theoretical and empirical predictions [11,12]. The present value of the mass excess of ^{17}Ne is in good agreement with previous measurements within the indicated errors. The evaluation by Wapstra *et al.* [11] is an average of the two experimental results from Refs. [3] and [4]. The isobaric multiplet mass equation prediction for the mass excess of ^{17}Ne was obtained using the mass excess of the ^{17}N ground state and lowest $T=\frac{3}{2}$ states of the ^{17}F and ^{17}O nuclei, which are the other members of the isobaric analog multiplet. The IMME analysis is discussed in Sec. V.

TABLE II. Comparison of the measurements and predictions of ^{17}Ne mass excess.

Authors	Mass excess (MeV)	Ref.
Experiment		
Present	16.453 ± 0.032	
Mendelson *et al.*	16.479 ± 0.050	[3]
Wozniak *et al.*	16.480 ± 0.050	[4]
Predictions		
IMME	16.496 ± 0.018	[a]
Wapstra	16.480 ± 0.050	[11]
Jänecke-Masson	16.62	[11]
Tachibana *et al.*	15.99	[11]
Comay-Kelson-Zidon	16.92	[11]
Pape-Antony	16.73 ± 0.33	[11]
Jänecke-Garvey-Kelson	16.630	[11]
Gul	16.630	[12]

[a]From mass excess of the other three members of the multiplet.

B. Angular distributions and the DWBA analysis

The experimental angular distributions of ^{6}He from the (^{3}He,^{6}He) reaction were obtained for eight levels in ^{17}Ne, and they are shown in Fig. 2 and Figs. 3(a)–3(e). As observed in these angular distributions, the measured differential cross sections are generally small, being in the range of a few tens of nb/sr for highly excited states. All the angular distributions, however, show distinct patterns at the forward angles, supporting the general feature of L dependence, as expected in direct multinucleon transfer reactions [13].

The spin-parity assignment of each state depends on the L assignment of the corresponding angular distribution. The assignment is made by comparing the experimental angular distribution with the calculated ones. Because both the target and ejectile nuclei have spin 0^+, any transition has a single value for the transferred orbital angular momentum (L) and two possible values for the transferred total angular momentum ($J=L\pm\frac{1}{2}$), except for an $L=0$ transition. The parity of the transition is given by $\pi=(-1)^L$. The analysis of the characteristic behavior at the forward angles in the angular distributions has been made in terms of the exact finite-range distorted wave Born approximation (DWBA), using the computer code TWOFNR [14]. The transitions should also satisfy the energy conservation rule [13]

$$\sum (2n_i+l_i)=2N_1+L_1+2\nu+\lambda \text{ for the target system,} \quad (1)$$

$$\sum (2n_i+l_i)=2N_2+L_2+2\nu+\lambda \text{ for the ejectile system,} \quad (2)$$

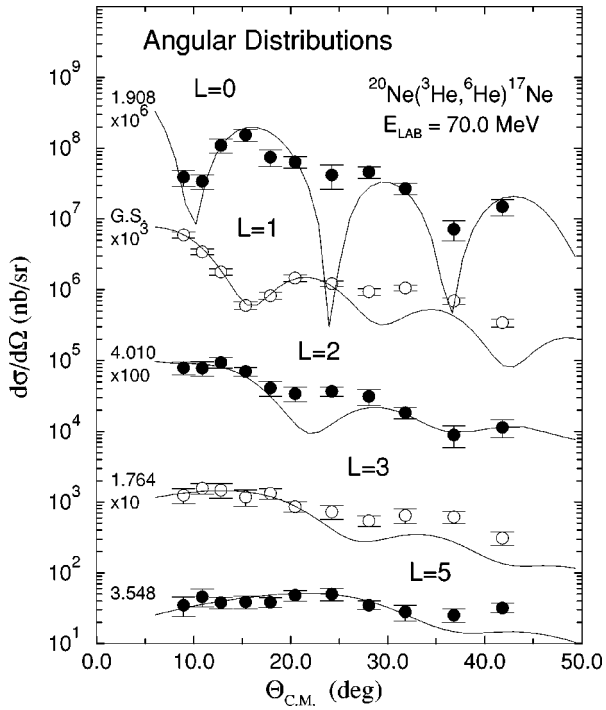

FIG. 2. Typical angular distributions of ^{6}He from the ^{20}Ne(^{3}He,^{6}He)^{17}Ne reaction for the states denoted. The curves are the results of DWBA calculations with the transferred angular momenta (L) indicated.

where n_i and l_i are the number of radial nodes (excluding the origin) and the orbital angular momentum of each constituent nucleon in the shell model, N_i and L_i are the number of radial nodes and the orbital angular momentum of the $3n$-cluster relative to the core, respectively, while ν and λ stand for the number of radial nodes and angular momentum of the internal motion in the $3n$-cluster. Since a direct one-step process of a $3n$-cluster transfer was assumed for the (^{3}He,^{6}He) reaction, the quantum numbers for the internal motion of all three identical fermions are $\nu=0$ and $\lambda=1$ for the transitions to the low-lying states. This implies that the $3n$ cluster in ^{6}He should have $J^\pi=\frac{3}{2}^-$ and $L_2=1(N_2=0)$ for the motion with respect to the ^{3}He core. Thus, for the low-lying states of the residual nucleus, the $3n$ cluster in ^{20}Ne should have $L_1=1(N_1=1)$ for the motion with respect to the ^{17}Ne core for $L=0$ transitions, where $\vec{L}=\vec{L}_1+\vec{L}_2$. For transitions with $L=1$ we have $2N_1+L_1=4$ for ^{20}Ne, which gives two possibilities for the quantum numbers of the relative motion, $L_1=2(N_1=1)$ or $L_1=0(N_1=2)$. These two possibilities for the quantum numbers did not change significantly the positions of the maxima and minima in the calculated angular distributions, but, since they give small changes in the relative intensity of the maxima, the set that better reproduced the experimental angular distributions was chosen.

The optical potential parameters in Table III, used in the calculations, were obtained from Ref. [15], for the incident channel, while those for ^{6}He were obtained from those of ^{6}Li also from Ref. [15]. These parameter sets were also used before in the analysis of angular distributions of the ^{24}Mg(^{3}He,^{6}He)^{21}Mg reaction [5]. For the bound state parameters of the $3n$ cluster, we adopted $r_0=1.32$ fm and $a=0.65$ fm in ^{20}Ne, and $r_0=1.58$ fm and $a=0.65$ fm in ^{6}He, where the radius was defined by $R=r_0A_{\rm core}^{1/3}$, and the potential depths were adjusted to reproduce the binding energies. These radius parameters are slightly larger than the value often used ($r_0=1.25$ fm). Although the radius parameters changed the amplitudes of the oscillations in the angular distributions, they did not modify the general pattern so largely.

In Fig. 2 some typical angular distributions of different L values are plotted together. The calculated angular distributions by DWBA show strong oscillation patterns and clear structures for different L. As can be seen in the figure, there is a smooth shift of the first minimum angles as a function of L ($\Theta_{\rm lab}=10°$ for $L=0$, $\Theta_{\rm lab}=15°$ for $L=1$, and so on), which enables us the L assignment. The calculated angular distributions show a dominant role of L, i.e., there was little change in shape at forward angles for the total angular momentum. As observed in the figure, the DWBA calculation reproduces reasonable well the oscillation phases of the experimental angular distributions. The fits deteriorate at larger angles as usual for transfer reactions [13]. These fits were obtained without modifying the optical potential parameters and the bound state potential parameters. Basically, the shift to backward angle of the first maximum and minimum for higher L defined the assignment, and by comparing the angular distributions with different L's one can observe how certain a particular assignment is.

The experimental angular distributions of the transitions for ^{17}Ne are also shown in Figs. 3(a)–3(e), where they are classified according to the L assigned for them. The general shapes of the angular distributions at forward angles and the oscillations phases (maximum and minimum angles) are reasonably well reproduced by the calculations with the L values denoted in the figures.

C. Spin parity based on L assignment

The transferred angular momentum, the parity, and the total angular momentum assigned for each state are summarized in Table I. The angular distribution of the ground state transition has the expected $L=1$ dependence behavior for a $J^\pi=\frac{1}{2}^-$ state [9]. The angular distribution of the 1.908 MeV state most likely has an $L=0$ dependence as shown in Fig. 3(a). However, this state is the weaker member of the unresolved doublet, and a small change in the shape of the peak could change the yield for this state especially for the most forward angles. Taking this into account we would not completely reject the possibility for an additional $L=2$ shape of the angular distribution based on the pattern of the backward angles points. Thus, for this state at 1.908 MeV we assigned $J^\pi=\frac{1}{2}^+$ with the possibility for $J^\pi=(\frac{3}{2}^+,\frac{5}{2}^+)$. When the transferred L is not zero, there are two choices of J for each L, as mentioned in the previous subsection. In this case, reasonable J's have been chosen using the known J^π's of the levels in the corresponding energy region in the mirror nucleus ^{17}N [16]. By using this procedure, we assigned $J^\pi=\frac{3}{2}^-$ for the state at 1.288 MeV, whose angular distribution has $L=1$ dependence. The angular distributions of the states at 2.651 and 4.010 MeV seem to have $L=2$ dependence, see Fig. 3(c). By comparing with the levels in ^{17}N we assigned $J^\pi=\frac{3}{2}^+$ for the state at 4.010 MeV. However, there

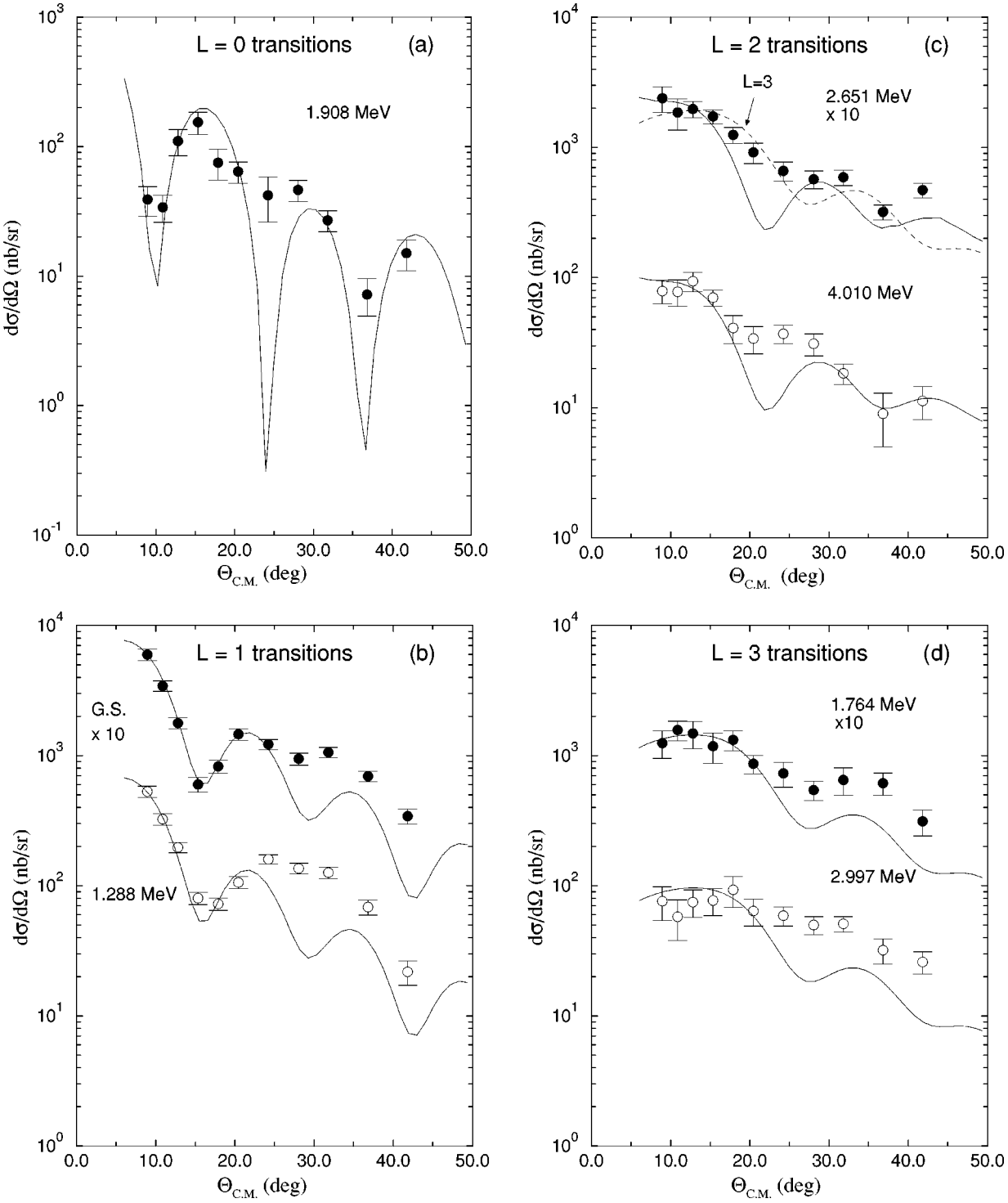

FIG. 3. Angular distributions of ^{6}He from the ^{20}Ne(^{3}He,^{6}He)^{17}Ne reaction for the states denoted, attributed to the transferred angular momenta indicated. The solid lines are the DWBA calculations for the corresponding L. Some angular distributions were multiplied by the factors indicated. (a) for $L=0$ transition, (b) for $L=1$ transitions, (c) for $L=2$ transitions, (d) for $L=3$ transitions, (d) for $L=5$ transitions.

is also a possibility that the angular distribution for the state at 2.651 MeV have $L=3$ dependence; thus, since we cannot clearly distinguish between these two possibilities, the ambiguity $J^{\pi}=(\frac{3}{2}^{+},\frac{5}{2}^{+},\frac{5}{2}^{-},\frac{7}{2}^{-})$ is left for the state at 2.651 MeV. This two possibilities for the angular momentum transferred could also indicate that this state might be a doublet. Since we have a rather moderate experimental resolution this possibility cannot be completely rejected. In our previous analysis [8] we considered this state at 2.651 as a doublet with two states at 2.623 and 2.765 MeV. In this case the angular distributions for these two possible states are shown in Fig. 4. As we can see in the figure, there is a strong indication that the angular distributions for these two states correspond to $L=3$ and $L=2$, respectively, in which case we would assign $J^{\pi}=\frac{5}{2}^{-},\frac{7}{2}^{-}$ for the state at 2.623 MeV and $J^{\pi}=\frac{3}{2}^{+},\frac{5}{2}^{+}$ for 2.765 MeV. The assignment of a doublet implies a signifi-

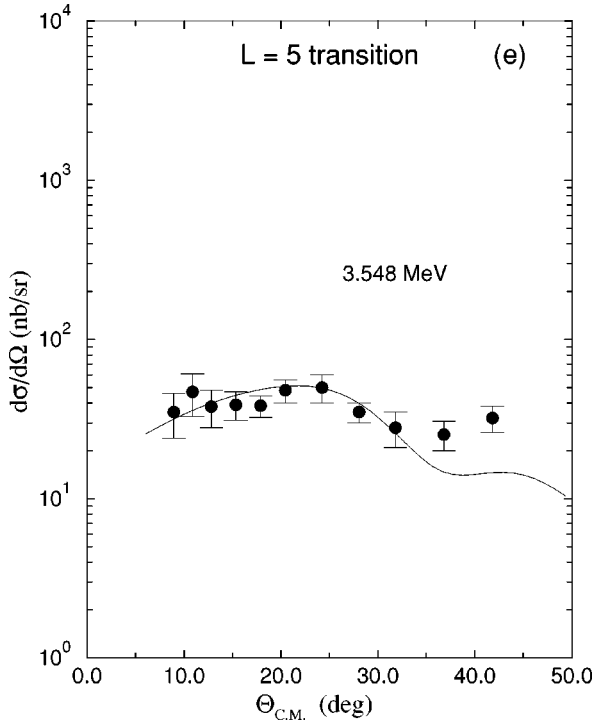

FIG. 3 (*Continued*).

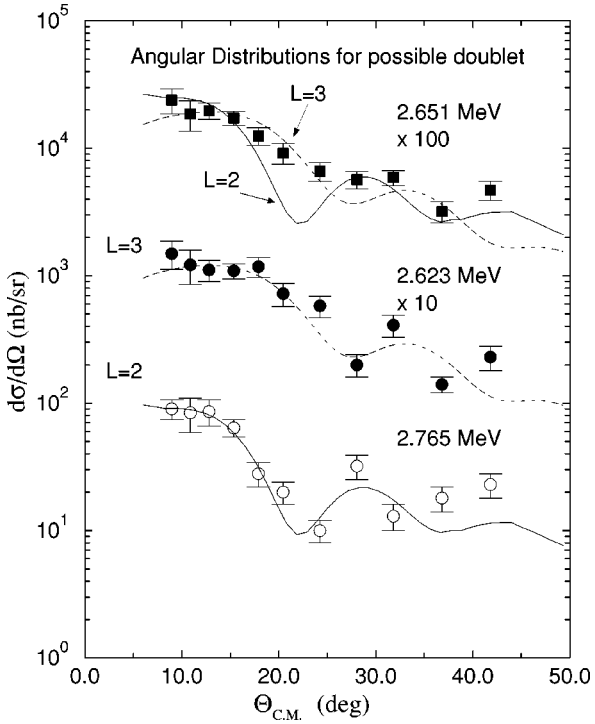

FIG. 4. Angular distribution of ^{6}He from the ^{20}Ne(^{3}He,^{6}He)^{17}Ne reaction for the state at 2.651 MeV considered as a single state and considered as a doublet with states at 2.623 and 2.765 MeV.

cant d coefficient for the IMME equation for the 2.765 MeV state, which we would assume as the fourth member of the $\frac{5}{2}^+$ quartet considering solely the spin assignment from the angular distribution. Since one cannot draw any conclusion for this possibility, from the IMME point of view it could, however, be an interesting subject to investigate further with better resolution if there is a doublet there and a large d term for the IMME in this nucleus.

The angular distributions of the 1.764 and 2.997 MeV transitions have $L=3$ dependence, see Fig. 3(d). The state at 2.997 MeV is considered to be the analog of the 3.129 MeV state in ^{17}N, and thus, $J^\pi=\frac{7}{2}^-$ is tentatively assigned for it. The state at 1.764 MeV is assigned $J^\pi=\frac{5}{2}^-$. Finally, the angular distribution of the 3.548 MeV state is fitted reasonably well by $L=5$, see Fig. 3(e). This state is considered to be the analog of the 3.629 MeV state in ^{17}N, and thus $J^\pi=\frac{9}{2}^-$ is assigned. These assignments are based solely on the L dependence of the angular distributions. The spin-parity assignments for these states are also discussed in Sec. V.

TABLE III. Optical and binding potential parameters.

set	V (MeV)	r_R (fm)	a_R (fm)	W_V[b] (MeV)	r_I (fm)	a_I (fm)	r_C (fm)
^{3}He+^{20}Ne	160.00	1.633	0.375	35.00	1.015	1.767	1.3
^{6}He+^{17}Ne	64.70	1.250	0.717	13.00	1.250	0.800	1.3
$3n+^{17}$Ne	[a]	1.32	0.65				
$3n+^{3}$He	[a]	1.58	0.65				

[a]The depth was adjusted to reproduce the binding energy.
[b]The imaginary potential is a volume-type Woods-Saxon potential for both systems.

IV. COMPARISON WITH SHELL MODEL CALCULATIONS

Shell model calculations performed for mass 17 nuclei [17–21] suggested that particle-hole excitations are important for the structure of low-lying states. Most of the calculations were based on the weak coupling model [22], in which the correlation between particles in the same major shell is of predominant importance and the particle-hole interaction is treated as a small perturbation. The low-lying negative parity states in $A=17$ nuclei arise mainly from coupling of a $p_{1/2}$ hole to positive parity states of mass 18. Besides these $2p$-$1h$ configurations, $4p$-$3h$ configurations are expected to play a role, while the positive parity states are expected to be $3p$-$2h$ and $5p$-$4h$. These works, however, differ with each other in the shell model space or in the number of configurations taken into account, and even in the choice of the residual interactions, which, as pointed out by Margolis and Takacsy [17], could have a large influence on the energy spectrum.

We here compared the experimental levels in ^{17}Ne with an extensive shell model calculation by Warburton and Millener [21] (see Fig. 5). Since their calculations do not include any Coulomb effect, they can be compared to the experimental energy levels in both ^{17}Ne and ^{17}N nuclei. They used a modified Millener-Kurath interaction (designated MK3) to describe the cross-shell interaction in which valence nucleon are active in several major shells simultaneously. This interaction is based on a multirange parametrization obtained by Hosaka *et al.* [23]. They defined the $(0s)^4(0p)^{12}(1s0d)$ configuration as $0\hbar\omega$. The low-lying negative parity levels in ^{17}N and ^{17}Ne are predominantly of $1\hbar\omega$ character. The model space for the positive-parity states included all pos-

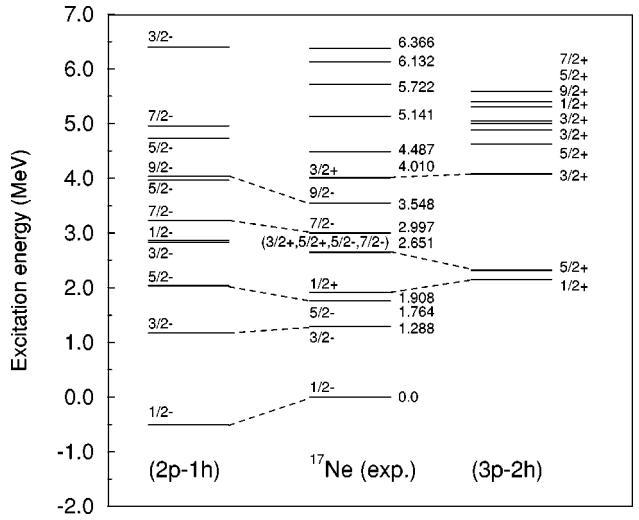

FIG. 5. Energy levels of ^{17}Ne. The theoretical predictions are taken from shell model calculations by Warbuton *et al.* The $2p$-$1h$ and $3p$-$2h$ model spectra are discussed in text.

sible $2\hbar\omega$ excitations as $(0s)^3(0p)^{12}(1s0d)^2$ and $(0s)^4(0p)^{11}(1s0d)^1(0f1p)^1$ configurations as well as the main $(0s)^4(0p)^{10}(1s,0d)^3$ configurations. In Fig. 5, we show the energy level scheme of ^{17}Ne compared with the $2p$-$1h$ and $3p$-$2h$ states predicted by this calculation. In the calculation the first ten odd-parity states are considered, according to the weak coupling model, to be mainly composed of

$$\pi p_{1/2}^{-1}\otimes[^{18}\mathrm{O}(0_1^+,2_1^+,4_1^+,2_2^+,0_3^+,3_1^+)]. \tag{3}$$

As may be seen in the figure there is a good one-to-one correspondence for the low-lying states in ^{17}Ne, indicating that the main configuration of these states is well characterized by the weak coupling model assumed. The exceptions are, however, the predicted additional $\frac{1}{2}^-$ and $\frac{3}{2}^-$ states, which do not have counterparts in the present ^{17}Ne spectrum. A $\frac{3}{2}^-$ state appears at 3.204 MeV in ^{17}N. However this state in ^{17}N has a very small spectroscopic factor in the ^{18}O$(d,^3$He$)^{17}$N reaction [20], which corroborates with the small spectroscopic factor calculated by Warburton and Millener [21]. In terms of the weak-coupling model these seconds $\frac{1}{2}^-$ and $\frac{3}{2}^-$ states would be $2p$-$1h$ configuration formed by coupling a p hole to the 0_3^+ and 2_2^+ states in $A=18$ nuclei, respectively. The low-lying positive parity states in $A=18$ nuclei have basically $2p$-$0h$ configuration. To describe correctly the excitation energies and electromagnetic properties of the positive-parity levels in $A=18$, ^{16}O core polarization has been required in shell model calculations [24,25]. This fact corresponds to introducing more particle-hole excitations such as $4p$-$2h$ for the wave functions of the positive-parity states in $A=18$. In particular, it was found in these shell model calculations that although the main configuration for 0_3^+ and 2_2^+ states in ^{18}Ne and ^{18}O is $2p$-$0h$, the $4p$-$2h$ component also has a large amplitude. Since the second $\frac{1}{2}^-$ and $\frac{3}{2}^-$ states are not populated in ^{17}Ne by the present $3n$-pickup reaction indicates that the two 0_3^+ and 2_2^+ parent states in $A=18$ could have predominantly a $4p$-$2h$ component.

V. IMME ANALYSIS

The ambiguity of the spin-parity assignment for the levels in ^{17}Ne, based on the L assignment, is eliminated by identifying analog states in the known level scheme of the mirror nucleus ^{17}N. However, to identify analog states in these nuclei sometimes it is necessary to consider signatures other than just their absolute energies and L assignment. One of these signatures is the isobaric multiplet mass equation (IMME). This equation relates the mass excess of the four members of an isobaric multiplet by the following expression:

$$M(A,T_z)=a+b\times T_z+c\times T_z^2+d\times T_z^3, \tag{4}$$

where T_z is the isospin projection and a, b, c, and d are the coefficients.

The most important coefficient to test the IMME equation is the d coefficient. This coefficient must be zero if the isospin is a good quantum number. In terms of the mass excess of the quartets it is given by

$$d=\frac{1}{6}\times\{M(\tfrac{3}{2})-M(-\tfrac{3}{2})-3\times[M(\tfrac{1}{2})-M(-\tfrac{1}{2})]\}, \tag{5}$$

where $M(T_z)$ is the mass excess of the nucleus with T_z. As is clear from the equation, the d coefficient is three times more sensitive to the mass difference between the $T_z=\pm\frac{1}{2}$ members of the multiplets than to that between the $T_z=\pm\frac{3}{2}$ members.

A. $T=\frac{3}{2}$ states in the $A=17$ multiplet

The coefficients of the IMME were obtained relating the mass excess of the $T=\frac{3}{2}$ states of the $A=17$ isobar multiplet. These coefficients were obtained for the $\frac{1}{2}^-$, $\frac{3}{2}^-$, $\frac{5}{2}^-$, $\frac{1}{2}^+$, $\frac{5}{2}^+$, and $\frac{7}{2}^-$ quartets. Here, we have assigned the state 2.651 MeV in ^{17}Ne as a state of the $\frac{5}{2}^+$ quartet.

The $T=\frac{3}{2}$ states in the other members of the $A=17$ multiplet have been well studied. In the ^{17}O and ^{17}F nuclei ($T_z=\pm\frac{1}{2}$) these states have been located mostly by observing proton and neutron induced resonances, where information on energy and spin-parity were obtained [26,27]. Figure 6 summarizes the present knowledge of the $T=\frac{3}{2}$ states in the $A=17$ isobar multiplet. The data on ^{17}N, ^{17}O, and ^{17}F are taken from the most recent compilation [16], while the data on ^{17}Ne are from the present results.

The identification of the first four quartets in this system seems very clear, since the spin parity of the states in these nuclei are well determined. However, concerning the states in the equivalent excitation energy region above 2.5 MeV, the identification of the analog states is not so clear. At the energy region around 2.5 MeV there is one positive parity state $\frac{5}{2}^+$ in ^{17}N, ^{17}O, and ^{17}F nuclei. In ^{17}Ne, the state in this region is the state at 2.651 MeV ($\frac{3}{2}^+,\frac{5}{2}^+,\frac{5}{2}^-,\frac{7}{2}^-$). Thus, we assume here that this state at 2.651 MeV in the ^{17}Ne is the fourth member of the $\frac{5}{2}^+$ quartet. In addition, in the previous compilation of data on ^{17}O [28], which was based on the data of Hinterberger *et al.* [27], the state at 14.286 MeV in ^{17}O was assumed to be a $T=\frac{3}{2}$ state. However, in a recent ex-

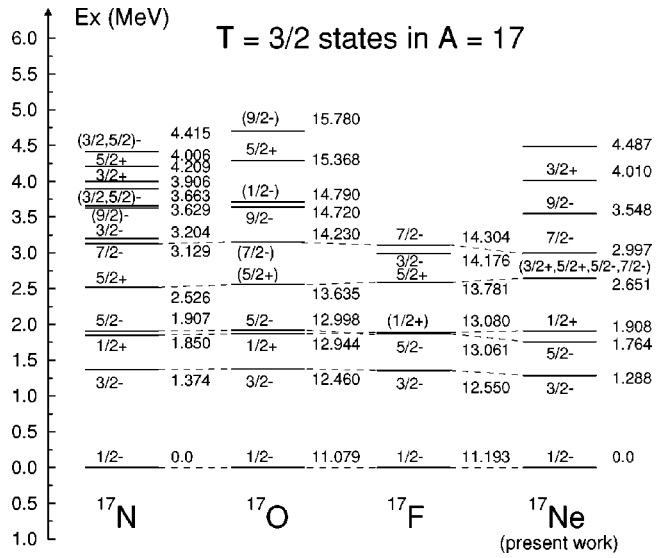

FIG. 6. $T=\frac{3}{2}$ energy levels in $A=17$ quartet. Excitation energies and J^{π} assignments for ^{17}N, ^{17}O, and ^{17}F are obtained from the compilation in Ref. [16], and for ^{17}Ne from the present experiment. The dashed lines correspond to the identified analog states.

periment [29] this state is found to be a $T=\frac{1}{2}$ state. Thus, the state at 3.204 MeV $\frac{3}{2}^-$ in ^{17}N has no analog in ^{17}O. It is also questionable to assume this state as the analog of the broad state at 14.176 MeV in ^{17}F. Although $J^{\pi}=\frac{3}{2}^-$ has been confirmed for the state at 14.176 MeV in ^{17}F [30], it is too apart in energy and its order is inverted relative to the $\frac{7}{2}^-$ state in ^{17}N. Moreover, the analog of this $\frac{3}{2}^-$ state in ^{17}F seems to be missing in this energy region in ^{17}Ne. The most plausible explanation for this situation is that there are missing states in this excitation energy region not only in ^{17}Ne but also in the other members of the multiplet. Missing states would be expected since spectroscopic data on ^{17}N, ^{17}O, and ^{17}F were obtained by using different reactions such as the stripping reaction, elastic scattering, or one-nucleon pickup reactions, whereas the present experiment on ^{17}Ne used a reaction which excited three-neutron hole states. Of course, since our experimental resolution was rather moderate, there remains a possibility that there is a missing state beneath the two states at 2.651 and 2.997 MeV in ^{17}Ne.

B. The systematics of the IMME coefficients

The coefficients a, b, c, and d of the IMME were obtained for the $\frac{1}{2}^-$, $\frac{3}{2}^-$, $\frac{5}{2}^-$, $\frac{1}{2}^+$, $\frac{5}{2}^+$, and $\frac{7}{2}^-$ quartets from the corresponding mass excess listed in Table IV. First, only the coefficients a, b, and c were obtained by using the experimental values of the mass excess of the three members of the multiplet (^{17}N, ^{17}O, and ^{7}F). By using these coefficients one can estimate the excitation energies for the analog states in ^{17}Ne. The predicted energies by the IMME for the states in ^{17}Ne are presented in the last column of Table I. All the energies are in very good agreement with the observed excitation energies in ^{17}Ne within the errors.

Using the mass excess of the four members of the multiplet in the IMME, one can determine the coefficients up to the d term. The coefficients obtained are listed in the second line for each state in Table IV. Apparently, inclusion of the ^{17}Ne data, and consequently the d coefficient, does not change the a, b, and c values significantly from the previous ones. The b, c, and d coefficients obtained are plotted in Fig. 7 as a function of excitation energy in ^{17}Ne. The b and c coefficients for the negative parity states have a weak linear dependence on excitation energy as

$$\frac{\Delta b}{\Delta Ex}=+15 \text{ keV/MeV} \quad \text{and} \quad \frac{\Delta c}{\Delta Ex}=-12 \text{ keV/MeV}, \tag{6}$$

which are much smaller than the prediction $+42$ keV/MeV and -18 keV/MeV for the b and c coefficients, respectively, for $A=17$ by Skwiersky *et al.* [26]. In their analysis only the energies of the ground and first excited states in ^{17}Ne were used, and they erroneously considered the state at 14.286 MeV in ^{17}O as $J^{\pi}=\frac{7}{2}^-$ instead of the state at 14.230 MeV. As mentioned before this state at 14.286 MeV in ^{17}O was found to be $T=\frac{1}{2}$ [29]. The systematics of the b coefficient for the negative parity states is opposite to the A dependence known previously, which is $b(A)\approx -0.2A$ for $A\leqslant 40$ [31].

TABLE IV. Mass excesses (in MeV) and the coefficients of IMME for the $T=\frac{3}{2}$ quartet of $A=17$. The numbers in parentheses are the errors in keV.

J^{π}	^{17}N ($T_z=\frac{3}{2}$)	^{17}O ($T_z=\frac{1}{2}$)	^{17}F ($T_z=-\frac{1}{2}$)	^{17}Ne ($T_z=-\frac{3}{2}$)	a (MeV)	b (MeV)	c (MeV)	d (keV)
$\frac{1}{2}^-$	7.871(15)	10.270(1)	13.145(2)	16.453(32)	11.648(2)	$-2.875(2)$	0.238(8)	
					11.651(3)	$-2.877(3)$	0.227(9)	7.2(6.0)
$\frac{3}{2}^-$	9.245(15)	11.657(1)	14.502(2)	17.741(33)	13.025(2)	$-2.845(2)$	0.217(8)	
					13.028(3)	$-2.847(3)$	0.207(9)	6.5(6.1)
$\frac{1}{2}^+$	9.721(15)	12.135(5)	15.032(5)	18.361(35)	13.527(5)	$-2.897(6)$	0.241(9)	
					13.526(5)	$-2.899(9)$	0.229(10)	8.5(7.0)
$\frac{5}{2}^-$	9.778(15)	12.189(1)	15.013(5)	18.217(34)	13.549(3)	$-2.824(4)$	0.207(8)	
					13.551(3)	$-2.825(7)$	0.198(10)	5.5(6.6)
$\frac{5}{2}^+$	10.397(15)	12.827(3)	15.733(5)	19.104(34)	14.220(3)	$-2.906(5)$	0.238(8)	
					14.221(4)	$-2.907(7)$	0.235(9)	1.8(6.9)
$\frac{7}{2}^-$	11.000(15)	13.422(2)	16.256(4)	19.450(34)	14.788(3)	$-2.834(4)$	0.206(8)	
					14.791(3)	$-2.836(4)$	0.193(9)	8.7(6.6)

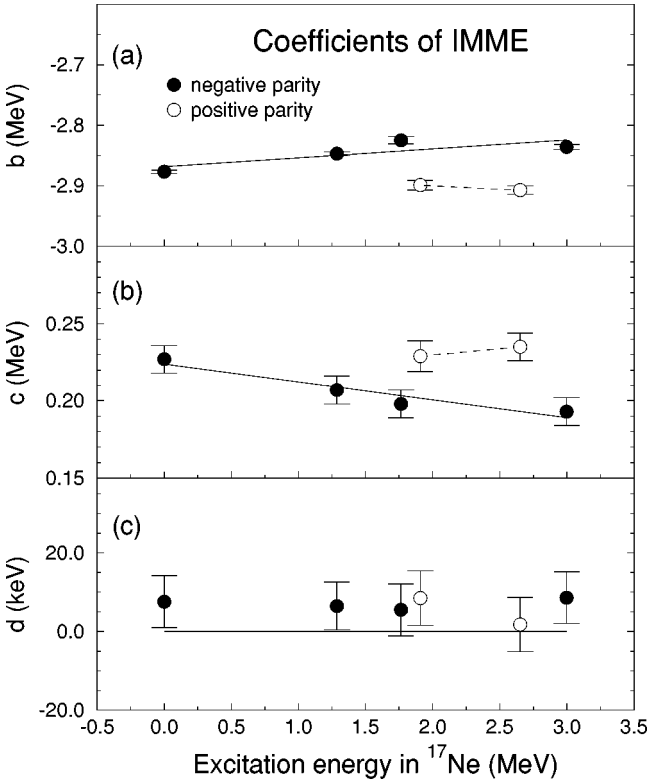

FIG. 7. The coefficients of the IMME as a function of excitation energy in ^{17}Ne; (a) the b coefficient, (b) the c coefficient, and (c) the d coefficient.

One can also see clearly that the coefficients of the positive parity states do not follow the systematics for the negative parity states. This seems to be related to the configurations of the states since the low-lying negative parity states in ^{17}Ne are predominantly $2p$-$1h$ configuration from $1\hbar\omega$ excitations while the positive-parity states are $3p$-$2h$ based on the $2\hbar\omega$ excitations [32].

Since data on excited state isobaric multiplets of $T=\frac{3}{2}$ were quite limited for light nuclei, excited state multiplets have received less attention than the ground state multiplets from a theoretical point of view. However, an extensive calculation of level displacement energy was made by de Meijer [33]. In his calculation he used different wave functions for protons and neutrons in a large shell model base. The results of this ambitious calculation for the first two negative and positive parity states in ^{17}Ne are presented in Table V. The calculation gives a larger difference between the experimental and calculated level displacement energies for the negative parity states and a smaller difference for the positive parity states. The difference of the calculated values from the experimental ones may be attributed to the fact that they used a fixed set of parameters for the Woods-Saxon potential for a large mass region, $A=9-28$. The level displacement energy is very sensitive to a small change in the radius parameter r_0; according to Bertsch [34], for $\Delta r_0=0.01$ fm one finds $\Delta E\approx 30$ keV for instance.

The d coefficients were obtained before for twenty-two isobaric quartets [35]. It was found that they are consistent with zero, as the upper limit of their absolute values is around 7 keV. The d coefficient determined here for the multiplets in $A=17$ nuclei are slightly positive nonzero values. The reason for the small deviation of nonzero values in average is partly due to the mass excess of ^{17}Ne determined here. Thus, the d coefficients obtained here for the excited states multiplets are consistent within the error with the d coefficients of the ground-state multiplet, since they are strongly correlated.

VI. LEVEL SHIFT

The level scheme of ^{17}Ne is shown in Fig. 5. Except for the ground state all levels are unbound for proton emission. As observed in the level scheme of ^{17}Ne the first positive parity state is the $\frac{1}{2}^+$ state at 1.908 MeV. This state comes lower in energy than the next possible positive parity state $\frac{5}{2}^+$ at 2.651 MeV.

Although nucleons occupy single-particle orbits from the bottom up to weakly bound states in a mean potential, the shell structure of proton or neutron rich nuclei can be different from that of stable nuclei. One of the intriguing consequences of this is the crossing or inversion of states, frequently observed in neutron-rich nuclei. Despite the fact that residual interactions in the nuclei lead to different level shifts state by state [36], the inversion of the $\frac{1}{2}^+$ and $\frac{5}{2}^+$ states or more specifically the strong lowering in energy of the $\frac{1}{2}^+$ state observed in some neutron-rich nuclei is not well understood yet.

Figure 8 shows the energy levels of the $\frac{1}{2}^+$ and $\frac{5}{2}^+$ states in the $N=7$ isotones measured from the lowest $\frac{1}{2}^-$ state, where we assumed the state at 2.651 MeV is the second positive-parity state in ^{17}Ne. These two states are unbound for proton emission, as the $\frac{1}{2}^+$ state in ^{17}Ne is unbound by only 408 keV. As can be observed in the figure, the $\frac{1}{2}^+$ state has lower energies toward the drip lines in both proton and neutron rich sides. In the extreme case of very neutron-rich nucleus ^{11}Be the two states are inverted. This inversion mechanism in ^{11}Be has been partly explained to be due to neutron-halo formation of the weakly bound valence neu-

TABLE V. The experimental level displacement energies of ^{17}F and ^{17}Ne analog states, and excitation energies in ^{17}Ne calculated by de Meijer *et al.* [33]. The numbers in parentheses are the errors in keV.

State	ΔE(exp) (MeV)	ΔE(calc) (MeV)	ΔE(exp)$-\Delta E$(calc) (keV)	Ex(exp) (MeV)	Ex(calc) (MeV)	Ex(exp)$-$Ex(calc) (keV)
$\frac{1}{2}^-$	4.090(32)	4.245	-155	0	0	0
$\frac{3}{2}^-$	4.021(33)	4.182	-161	1.288(8)	1.289	1
$\frac{1}{2}^+$	4.111(35)	4.053	$+58$	1.908(15)	1.667	$+241$
$\frac{5}{2}^+$	4.153(34)	4.154	-1	2.651(12)	2.486	$+165$

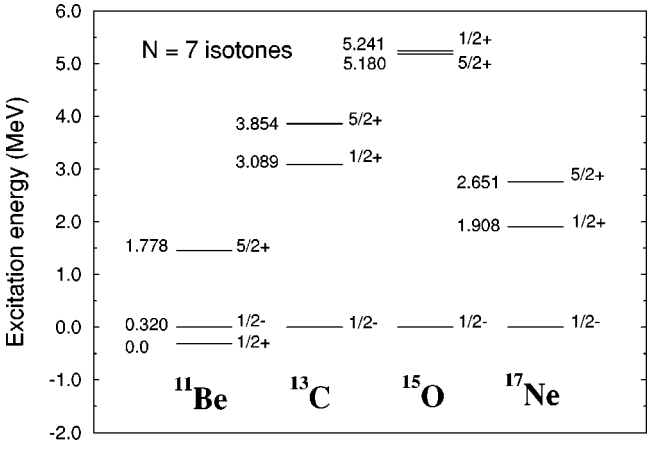

FIG. 8. Energy difference between the $\frac{1}{2}^+$ and $\frac{5}{2}^+$ states in the $N=7$ isotones spanned from the neutron-rich to the neutron-deficient nuclei. The lowest $\frac{1}{2}^-$ states of each nucleus are normalized to zero. The excitation energies for the states in ^{15}O and ^{13}C are from Ref. [37].

tron. Although this inversion has been a long standing problem pointed out by Talmi [38], it is not well understood yet. Tanihata *et al.* [39] have shown that in a mean field shell model calculation, the potential extends more in the surface for the $2s$ orbital than for the orbits with centrifugal barriers near the threshold. If these low-lying states are of largely single-particle nature, the large energy shift of the $\frac{1}{2}^+$ state in neutron-rich nuclei can be understood partly as a property of a loosely bound system with a diffuse surface. In principle, the formation of a proton-halo in proton-rich nuclei can be difficult due to the Coulomb repulsion between the proton and the nucleus, but on the other hand, the absence of centrifugal barrier for an *s* state can help holding the last nucleon. Of course these are still open questions and more detailed spectroscopic studies on such states in proton-rich nuclei may bring valuable information. In particular, it is interesting to investigate if the lowering of the $\frac{1}{2}^+$ state has some relation to the largest interaction radius among the $A=17$ isobars observed for ^{17}Ne [2].

VII. SUMMARY

The structure of ^{17}Ne nucleus has been investigated by the ^{20}Ne(^{3}He,^{6}He)^{17}Ne reaction. This reaction has been shown to proceed predominantly through a direct three-neutron transfer mechanism. Thirteen levels were identified in ^{17}Ne and the angular distributions for eight of them were measured. The transferred-orbital-angular-momentum dependence is clearly observed in the angular distributions, which enables spin and parity assignments for several levels.

The experimental ^{17}Ne level scheme is in reasonable agreement with the shell model calculation based on the weak coupling model, although the nuclear structure of these levels is not yet completely understood. The $\frac{1}{2}^+$ state at 1.908 MeV is the first positive parity state, while the possible next positive parity state $\frac{5}{2}^+$ is at 2.651 MeV. Although the spin-parity assignment based on the angular distribution for the 2.651 MeV state is not so clear, the systematic of the IMME indicates that this state is the most reasonable candidate for the $\frac{5}{2}^+$ analog states quartet. And, since we expect that these states are of largely single particle character, one may conclude that the *s* orbit comes lower than the *d* orbit in energy. Moreover, the lowering in energy of the $\frac{1}{2}^+$ state in association with weak binding effects in nuclei with diffuse surface [38] can be an interesting point for further investigation in proton-rich nuclei.

The inclusion of data on the nuclear structure of ^{17}Ne to the known $T=\frac{3}{2}$ state in $A=17$ isobar multiplet allowed the identification of six quartet analog state. An extensive IMME analysis for these states up to $d\times T_z^3$ term of the equation has been made. In the analysis an excitation energy dependence for the coefficients of the IMME, including the cubic term *d* was observed. The different systematics of the *b* and *c* coefficients observed for the positive and negative parity states seem to be related to the shell model configurations expected for these states. Detailed theoretical analysis of the present systematics of the IMME coefficients for the $A=17$ system can be found in Ref. [32].

ACKNOWLEDGMENTS

The authors are grateful to the cyclotron crew of the Center for Nuclear Study. The first author (V.G.) was financially supported by the Pró-reitoria de Pesquisa e Pós-Graduação da UNIP (Universidade Paulista) and FAPESP (Fundação de Amparo a Pesquisa do Estado de São Paulo). All the DWBA calculations were made using FACOM computer of the INS. This work was partly supported by the Grant-in-Aid for Scientific Research on the Priority Areas (Grant No. 05243103) of the Ministry of Education, Science, Sports and Culture in Japan.

[1] K. Riisager, A. S. Jensen, and P. Moller, Nucl. Phys. **A548**, 393 (1992).
[2] A. Ozawa, T. Kobayashi, H. Sato, D. Hirata, I. Tanihata, O. Yamakawa, K. Omata, K. Sugimoto, D. Olson, W. Christie, and H. Wieman, Phys. Lett. B **334**, 18 (1994).
[3] R. Mendelson, G. J. Wozniak, A. D. Bacher, and J. M. Cerny, Phys. Rev. Lett. **25**, 533 (1970).
[4] G. J. Wozniak, R. Mendelson, J. M. Loiseaux, and J. Cerny, Lawrence Berkeley Laboratory Report No. LBL-1666, 1972, p. 76.
[5] S. Kubono, Y. Funatsu, N. Ikeda, M. Yasue, T. Nomura, Y. Fuchi, H. Kawashima, S. Kato, H. Miyatake, H. Orihara, and T. Kajino, Nucl. Phys. **A537**, 153 (1992).
[6] M. H. Tanaka, S. Kubono, and S. Kato, Nucl. Instrum. Methods Phys. Res. **195**, 509 (1982).
[7] S. Kato, M. H. Tanaka, and T. Hasegawa, Nucl. Instrum. Methods **154**, 19 (1978).
[8] V. Guimarães, S. Kubono, M. Hosaka, N. Ikeda, M. H. Tanaka, T. Nomura, I. Katayama, Y. Fuchi, H. Kawashima, S. Kato, H. Toyokawa, C. C. Yun, T. Niizeki, T. Kubo, and M.

Ohura, Z. Phys. A **353**, 117 (1995).
[9] J. C. Hardy, J. E. Esterl, R. G. Sextro, and J. Cerny, Phys. Rev. C **3**, 700 (1971).
[10] *The Stopping and Ranges of Ions in Matter*, edited by J. F. Ziegler (Pergamon, New York, 1980), Vols. 1 and 5.
[11] A. H. Wapstra, J. Britz, and Pape, At. Data Nucl. Data Tables **39**, 281 (1988).
[12] K. Gul, J. Phys. Soc. Jpn. **44**, 353 (1978).
[13] A. Arima and S. Kubono, *Treatise on Heavy-ion Science*, edited by D. A. Bromley (Plenum, New York, 1984), Vol. 1, Chap. 6.
[14] M. Igarashi (unpublished).
[15] C. M. Perey and F. G. Perey, Nucl. Data Tables **10**, 539 (1972).
[16] D. R. Tilley, H. R. Weller, C. M. Cheves, Nucl. Phys. **A564**, 1 (1993), and references therein.
[17] B. Margolis and N. de Takacsy, Can. J. Phys. **44**, 1431 (1966).
[18] B. S. Reehal and B. H. Wildenthal, Part. Nuclei **5**, 137 (1973).
[19] W. D. M. Rae, N. S. Godwin, D. Sinclair, H. S. Bradlow, P. S. Fisher, J. D. King, A. A. Pilt, and G. Proundfoot, Nucl. Phys. **A319**, 239 (1979).
[20] G. Mairle, G. J. Wagner, K. T. Knofle, Liu Ken Pao, H. Riedesel, V. Bechtold, and L. Friedrich, Nucl. Phys. **A363**, 413 (1981).
[21] E. K. Warburton and D. J. Millener, Phys. Rev. C **39**, 1120 (1989).
[22] P. S. Ellis and T. Engeland, Nucl. Phys. **A144**, 161 (1970).
[23] A. Hosaka, K. I. Kubo, and H. Toki, Nucl. Phys. **A444**, 76 (1985).
[24] J. B. McGrory and B. H. Wildenthal, Phys. Rev. C **7**, 974 (1973).
[25] A. P. Zuker, Phys. Rev. Lett. **23**, 983 (1969).
[26] B. M. Skwiersky, C. M. Baglin, and P. D. Parker, Phys. Rev. C **9**, 910 (1974).
[27] F. Hintergerber, P. von Rossen, S. Cierjacks, G. Schmalz, D. Erbe, and B. Leugers, Nucl. Phys. **A322**, 93 (1981).
[28] F. Ajzenberg-Selove, Nucl. Phys. **A460**, 1 (1986), and references therein.
[29] K. G. McNeill and J. W. Jury, Phys. Rev. C **42**, 2234 (1990).
[30] F. M. Khan, J. Lowe, J. M. Nelson, and A. R. Barnett, Nucl. Phys. **A322**, 33 (1979).
[31] M. S. Antony, J. Britz, J. B. Bueb, and A. Pape, At. Data Nucl. Data Tables **33**, 447 (1985).
[32] S. Nakamura, V. Guimarães, and S. Kubono, Phys. Lett. B **416**, 1 (1998).
[33] R. J. de Meijer, H. F. J. van Royen, and P. J. Brussaard, Nucl. Phys. **A164**, 11 (1971).
[34] G. F. Bertsch, Phys. Rev. **174**, 1313 (1968).
[35] W. Benenson and E. Kashy, Rev. Mod. Phys. **51**, 527 (1979).
[36] A. C. Mueller and B. M. Sherril, Annu. Rev. Nucl. Part. Sci. **43**, 529 (1993).
[37] F. Ajzenberg-Selove, Nucl. Phys. **A523**, 1 (1991), and references therein.
[38] I. Talmi and I. Unna, Phys. Rev. Lett. **4**, 469 (1960).
[39] I. Tanihata, D. Hirata, and H. Toki, Nucl. Phys. **A583**, 769c (1995).